

Conf-941267--2

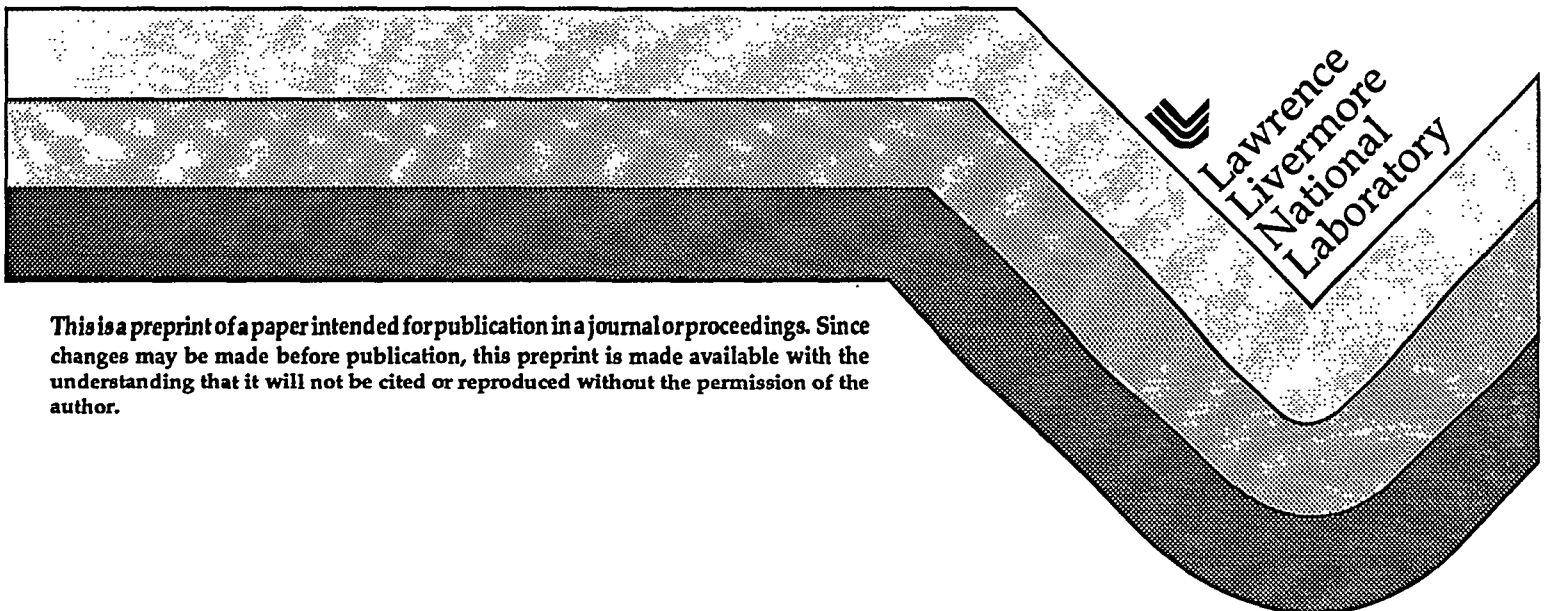
UCRL-JC-119608

**Growth Morphology of Vicinal Hillocks
on the {101} Face of KH_2PO_4 :
Evidence of Surface Diffusion**

T. A. Land
J. J. De Yoreo
J. D. Lee
J. R. Ferguson

This paper was prepared for submittal to the
Proceedings of the Materials Research Society
Boston, MA
December 5-9, 1994

January 10, 1995



This is a preprint of a paper intended for publication in a journal or proceedings. Since changes may be made before publication, this preprint is made available with the understanding that it will not be cited or reproduced without the permission of the author.

DISCLAIMER

This document was prepared as an account of work sponsored by an agency of the United States Government. Neither the United States Government nor the University of California nor any of their employees, makes any warranty, express or implied, or assumes any legal liability or responsibility for the accuracy, completeness, or usefulness of any information, apparatus, product, or process disclosed, or represents that its use would not infringe privately owned rights. Reference herein to any specific commercial product, process, or service by trade name, trademark, manufacturer, or otherwise, does not necessarily constitute or imply its endorsement, recommendation, or favoring by the United States Government or the University of California. The views and opinions of authors expressed herein do not necessarily state or reflect those of the United States Government or the University of California, and shall not be used for advertising or product endorsement purposes.

DISCLAIMER

Portions of this document may be illegible in electronic image products. Images are produced from the best available original document.

GROWTH MORPHOLOGY OF VICINAL HILLOCKS ON THE {101} FACE OF KH_2PO_4 : EVIDENCE OF SURFACE DIFFUSION

T. A. Land, J.J. De Yoreo, J.D. Lee and J. R. Ferguson
Lawrence Livermore National Laboratory, Livermore, CA 94550

ABSTRACT

The growth morphologies of vicinal hillocks on KH_2PO_4 {101} surfaces have been investigated using atomic force microscopy. Both 2D and spiral dislocation growth hillocks are observed on the same crystal surface at supersaturations of $\sim 5\%$. Growth occurs on monomolecular 5 Å steps both by step-flow and through layer-by-layer growth. The distribution of islands on the terraces demonstrate that surface diffusion is an important factor during growth. Terraces that are less than the diffusion length do not contain any islands. This, together with the length scale of the inter island spacing and the denuded zones provide an estimate of the diffusion length. In situ experiments at very low supersaturation ($\sim 0.1\%$) show that growth is a discontinuous process due to step pinning. In addition, in situ images allow for the direct determination of the fundamental growth parameters α , the step edge energy, and β , the kinetic coefficient.

INTRODUCTION

In recent years the nanometer-scale morphology of crystalline surfaces has received considerable attention. This interest is due to the large role that the nanoscale features play in the control of materials properties and performance. Most studies have considered the growth of surfaces by molecular beam epitaxy or chemical vapor deposition where the system is generally far from equilibrium both in terms of the flux of impinging molecules and the chemical potential. It has been shown both theoretically [1,2] and experimentally [2] that, in this regime, growth progresses either by step-flow at pre-existing steps on vicinal surfaces or through layer-by-layer and multi-layer growth on nucleating islands. For example, during the growth of Si at typical deposition conditions, the critical nucleus consists of only a single atom, as shown in scanning tunneling microscopy studies [3]. Few studies [4-8] have given attention to the nano-meter scale morphology of single crystal surfaces grown at low-to-moderate supersaturation despite the fact that most bulk single crystals are grown in this manner. In this regime stable islands consist of tens of molecules and the classic dislocation controlled mode of growth first described by Burton, Cabrera and Frank (BCF) [9] should be applicable.

Recently, we reported AFM results on the growth morphology of KH_2PO_4 (KDP) grown at low to moderate supersaturations [4]. It was shown that the {101} surface advances on monomolecular steps even on dislocation-induced vicinal hillocks where the Burgers vector exceeds one unit step. Local supersaturations were calculated from the measured Burgers vectors and the hillock slopes. These results were then compared to the predictions of BCF-type theories. For Burgers vectors of more than one unit step, the hillocks were observed to contain hollow cores. The size of these cores compared well with theoretical predictions, and the shape demonstrated that the step edge energy is isotropic. We showed that, at moderate supersaturations ($\sim 5-10\%$), the growth of KDP {101} surfaces occurs both on dislocation induced steps and on islands formed by 2D nucleation.

Here we explore two additional aspects of KDP growth: the interaction of steps with islands at supersaturations (σ) of 5-10%, and the dynamics of step motion at very low supersaturation ($\sigma \sim 0.1\%$). We find that island growth competes with step-flow when the inter-island spacing is comparable to the terrace width, and that on sufficiently large terraces, the regions near the step edges are devoid of islands. The distribution of islands shows that surface diffusion plays an important role in determining the rate of crystallization of KDP-like crystals. The length

scale of the inter island spacing and the denuded zones provide an estimate of the diffusion length. In situ experiments at low supersaturation ($\sim 0.1\%$) show that growth is a discontinuous process due to step pinning. In addition, in situ images allow for the direct determination of the fundamental growth parameters α , the step edge energy, and β , the kinetic coefficient.

RESULTS AND DISCUSSION

Ex situ samples were grown in stirred solutions at temperatures near 305 °K and were drawn from solution through a hexane bath to preserve the nascent surface structures. The samples were then transferred to the AFM for analysis. In situ experiments were performed using a commercially available Digital Instruments fluid cell [10]. $\{101\}$ plates of KDP were used as seeds for both types of experiments.

Hillock geometry

Vicinal hillocks on the $\{101\}$ face of KDP exhibit an asymmetric triangular anisotropy related to the crystal structure. Two AFM images of hillocks illustrating this anisotropy are shown in Figs. 1a and 1b. In the discussion that follows, the steepest slope is referred to as sector 1 and the shallowest as sector 3. Fig. 1b is a higher resolution image of the top portion of a hillock. This hillock is about 50 microns in size and consists of a double spiral of terraces generated by a dislocation for which the component of the burgers vector perpendicular to the face has a net number of steps $m=2$. The height of the steps is 5 Å which, within experimental error, is equal to half the unit cell parameter of 10.2 Å in the $\langle 101 \rangle$ direction. This corresponds to the distance between K-planes and is one monomolecular layer in thickness.

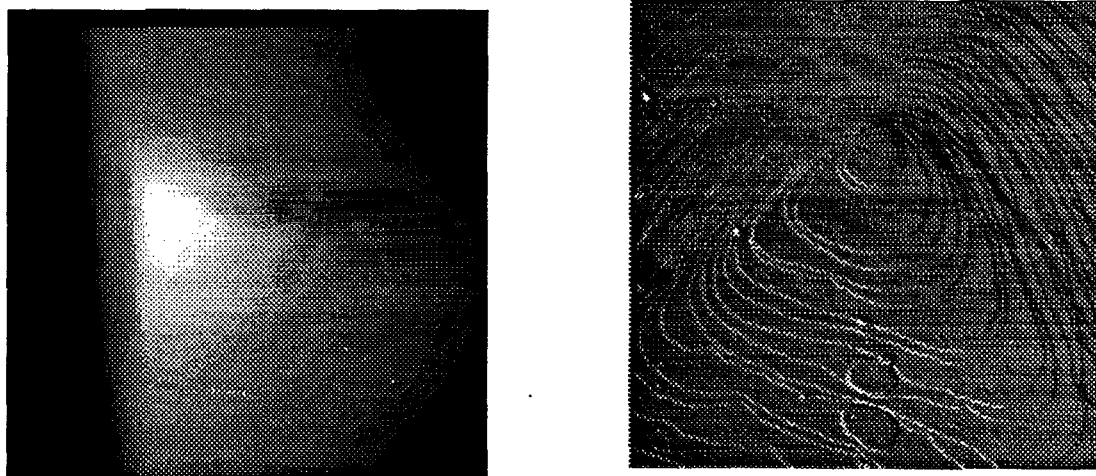


Fig. 1a - 35x35 μm AFM image of a vicinal hillock on the $\{101\}$ face of KDP.
1b - 5.3x5.3 μm image of a growth hillock on the $\{101\}$ face of KDP.

We have previously shown that there are two types of growth hillocks found on the $\{101\}$ surface of KDP [4]. One type of hillock appears to be formed by 2D nucleation, the other is generated by screw dislocation growth. At dislocations with Burgers vectors for which $m>1$, we find that the growth hillocks exhibit hollow cores (see Fig. 1b). All hollow cores that were observed were circular in cross section demonstrating that the free energy of the step riser is isotropic and that the anisotropy in the hillock geometry is due not to the energetics of the monomer-step interactions, but to kinetic constraints on adsorption and diffusion, (i.e. anisotropy in the kinetic coefficient, β). Measurement of the core radii are in good agreement with theoretical predictions provided inelastic effects are considered.

All spirals that were observed were composed of single steps regardless of the Burgers vector. Near the tops of spirals for which $m > 1$, the steps emerged from the dislocations in groups of order m (see Fig. 1b), while far from the hillock top the steps were observed to have approximately equal spacing. This step homogenization with time is evidence for the existence of a Schwoebel barrier [11,12] as well as the importance of surface diffusion and shows that the diffusion length of adsorbed monomer is comparable to the terrace width. Steps above broad terraces can draw monomer from larger areas than those above narrow terraces and therefore they move more rapidly, eventually equalizing the inter-step distances. The importance of surface diffusion is further discussed below.

2D island growth

Growth on the $\{101\}$ faces of KDP is not confined to growth spirals, in fact, we usually find that both 2D and spiral growth hillocks co-exist on the same crystal. Fig. 2a shows an AFM image of one of a number of hillocks on the surface of a crystal grown at $\sigma \sim 5\%$ that consist of flat-lying, single-layer islands. As is clear from the higher resolution image shown in Fig. 2b, there is no evidence for a screw dislocation at the top of such hillocks indicating that these islands have formed through 2D nucleation.

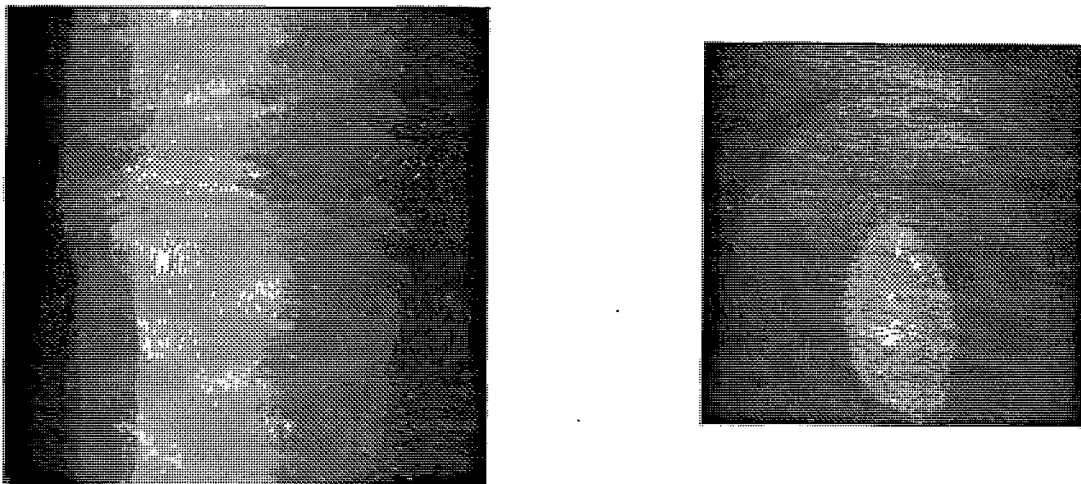


Fig. 2 - (a) 5.4x5.4 μm AFM image of typical hillock on KDP $\{101\}$ at which no dislocations are observed. (b) Higher resolution 715x715 nm image of one such hillock showing the topmost island for which the radius is 42 nm.

Two dimensional nucleation also occurs on the inter-step terraces of these hillocks as shown in Fig. 3. The average island spacing is controlled both by the degree of supersaturation and the surface diffusion length, x_s . Because the supersaturation is the same on all sectors of the hillock, the presence or absence of islands must depend on the size of the average terrace width relative to x_s . Fig. 3 shows the common occurrence of islands near the boundary between sectors 2 and 3 of the hillock in Fig. 2a. While most of the steps have approximately equal spacings, near the center of the image, one of the steps has stopped advancing and is being overgrown by the upper step. As a result, the lower terrace has broadened and is covered by islands which are one to three layers in thickness. The other terraces contain smaller, single step-height islands whose average spacing is 270 nm. The terraces themselves have average widths of 390 nm on sector 2 and 840 nm on sector 3. In comparison, the terraces of even the shallowest dislocation induced hillock ($m=1$) are only about one third as wide on the corresponding sectors and no islands are observed on these hillocks. No islands are observed on sector I for which the average terrace width is only 150 nm. We conclude that, for these growth conditions, the surface diffusion length, x_s , is on the order of 200nm or 400 lattice sites. On terraces that are narrower than this, the steps act as sinks and no island formation takes place. Thus this hillock exhibits the transition from step-flow to layer-by-layer growth. When the average terrace width is greater than the island

separation, growth proceeds layer-by-layer on nucleating islands. But when the converse is true, growth occurs by step-flow [1,2].

It is also interesting to note that the larger islands on the steps in Fig. 4 have an elongated shape with the long edge running parallel to the step edge in sector 3 and perpendicular to the step edge in sector 2. The shape of the islands is indicative of anisotropic surface diffusion or step edge energy.

Surface diffusion

Vekilov et al. [13] concluded that surface diffusion is an important mechanism in determining the rate of advancement of steps on KDP-like crystals and that the hillock anisotropy is due to differences in jump distances for diffusion on the three sectors, although little is known about the mechanism of diffusion or the diffusing species. Our results indicate that surface diffusion is an important mechanism and are in stark contrast to the conclusions of Gratz et al. [8] with respect to surface diffusion during the growth of calcite. However, we believe that the hillock and the island shape is not simply due to a difference in jump distance as suggested in ref. 13, as it is possible to reach all three step edges by a series of equal length jumps [14]. The anisotropy must therefore be controlled by the energetics of the jump barriers in the various directions. We are currently in the process of modeling the details of KDP surface diffusion [14].

The distribution of islands on the terraces in Fig. 4 demonstrate the importance of surface diffusion during the growth of KDP. In this image of a crystal grown at $\sim 7\%$ supersaturation, the larger terraces are covered with islands with the exception of the denuded zones at both the ascending and descending edges. The islands seen with the AFM range in size from $20-100$ nm with an average spacing of ~ 70 nm. When the terraces are < 100 nm no islands are present. The width of the denuded zone at the ascending step edge is ~ 100 nm and is slightly larger at the descending step edge. The presence of denuded zones, as well as other characteristics of this surface, are clear evidence of surface diffusion [3]. We suggest that this surface is generated by the following process: Monomer units are continually being adsorbed on the surface leading to the formation of a supersaturated 2D lattice gas. The system is driven to reduce the supersaturation by incorporating the excess monomer into the lattice either by 2D island formation or incorporation at steps. The step edge acts as a sink for the diffusing species. Any monomers landing within the diffusion length of the step are incorporated into the step before they have a chance to meet other monomers and form islands thereby creating a bare or denuded zone. The width of the denuded zone is related to the diffusion length. Further out on the terrace the density of monomer continues to build up, since there are no sinks. Eventually there are enough diffusing species to form critical nuclei. Once stable islands have formed they can grow by capturing diffusing species. The distance between the islands is related to the length that a monomer travels before being captured.

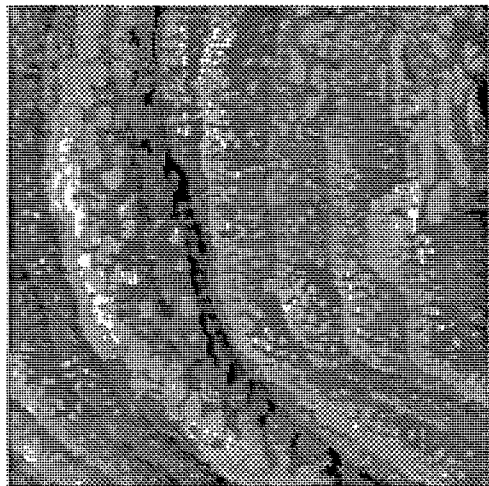


Fig. 3 - A $6.3 \times 6.3 \mu\text{m}$ area near the boundary between sectors 2 and 3 of hillock in fig. 2a. Note the presence of islands on all terraces.

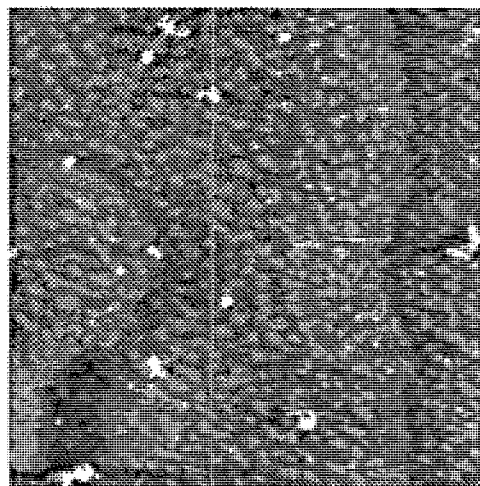


Fig. 4 - $1.8 \times 1.8 \mu\text{m}$ image of terraces covered with islands and a ~ 100 nm denuded zone at the step edge.

A dynamic process of nucleation, growth and dissolution of islands occurs on the surface and monomer units are continually adsorbing and desorbing from islands. As the step edge advances, monomer units desorbing from islands in the vicinity of the step are captured by the step which acts as a sink to diffusing species. This process is responsible for perpetuating the denuded zone at the ascending step edge. The denuded zone on the upper terrace (the descending edge) may be formed by one of two mechanisms. One possibility is that there is little or no asymmetry in the barrier to diffusion over a step edge, i.e., there is no appreciable Schwoebel barrier [11] and monomer landing within the diffusion length on both sides of the step are incorporated. The other more likely possibility is that, as the step edge advances, a fresh surface is exposed on the upper terrace edge. If nucleation is slower than the rate of step advancement then a denuded zone would be formed. The length scale of the inter island spacing and the denuded zones indicate that the diffusion length near 305 °K and 7 % supersaturation is on the order of 100 nm. This is further supported by the absence of islands on terraces that are <100 nm.

In situ

Another aspect of our work involves the in situ investigation of growth dynamics at low supersaturation. The series of six 2x2 μm images shown in Figs. 5a-e show the advancement of a series of steps at a supersaturation of ~0.1± 0.05 %. From the progression of these images, one can see that growth is a discontinuous process due to step pinning. The steps are described starting from left to right and adding to this number as new steps grow into the image from the right. Fig. 5a shows four terraces exposed with three straight steps in the image. In Fig. 5b step number 1 is beginning to bulge out from a pinning site located near the center of the image, steps 2 and 3, while bunched together, are still straight steps at this time. In Fig. 5c steps 2 and 3 are now following the contour of step 1 and are being pinned between the same two locations (one pinning site is below the frame the image). A new step 4, with a large ~25 nm particle acting as a pinning site, has emerged at the right side of the image. In Fig. 5d steps 1-3 have broken away from the pinning site below the frame of the image, and an additional pinning site has formed very near the first one. While steps 2 and 3 are advancing, step 1 has become pinned between this site and one to the left of the image. Step 4 is flowing around its pinning site. In Fig. 5e steps 1,2 and 3 have broken through the second pinning site and have become bunched again. Step 4 has developed a new pinning site and four new steps have entered lower left-hand side of the image. These images show how the persistence of strong pinning sites and the release of weaker ones effects growth on the nanometer scale. While most of the pinning sites and impurities are unresolvable, at least one consists of an adsorbed particle of about 25 nm (see arrow on Fig. 5). This particle was observed in a large number of sequential images and, even with the passage of 10 steps the particle remained the same height on the surface. This shows that the particle is displaced upward as the steps move through. Other instances where a particle is observed to be in the same place in series of images where the steps simply move under the particle without being pinned have been observed. Further experiments with various concentrations of known impurities are planned to further understand how impurities are incorporated in the crystal and how they influence growth.

These in-situ images are important because they provide a way to directly determine several fundamental parameters of KDP. The following equation relates the critical radius, r_c , to the supersaturation σ [9]:

$$r_c = \omega\alpha/kT\sigma \quad (1)$$

where ω is the specific molecular volume and equals $9.68 \times 10^{-23} \text{ cm}^3$ for KDP, α is the step edge energy per unit step height, k is Boltzman's constant and T is the temperature, we are able to determine the fundamental parameter α . From measurements of the radius of curvature of the pinned steps in the image and use of equation (1), we calculate the step edge free energy α to be $33 \pm 17 \text{ J/cm}^2$. This compares to a literature value of 24 J/cm^2 [15]. (Further experiments are planned to provide greater statistics). We are also able to determine the kinetic coefficient β by directly measuring the velocity of the unpinned steps in these images and using the relationship $v = \beta\sigma$ [13]. From these measurements, we calculate the kinetic coefficient β to be $\sim 20 \text{ } \mu\text{m/sec}$. Further experiments are planned at various supersaturations and temperatures to elicit a greater base of information about the fundamental growth parameters of KDP.

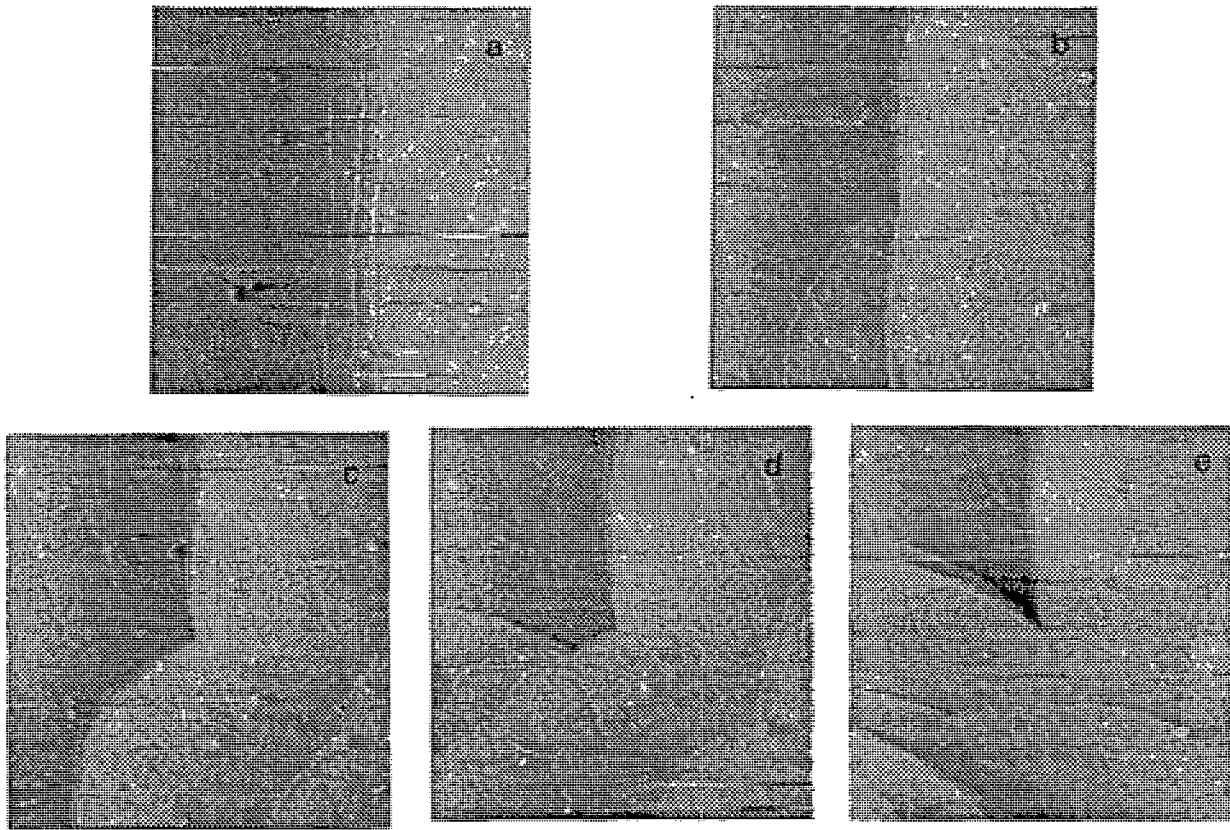


Fig. 5 (a-e) - A series of $2 \times 2 \mu\text{m}$ images collected in situ on a growing KDP $\{101\}$ surface at $T=26.5 \text{ }^\circ\text{C}$ and $\sigma \approx 0.1 \%$. Collection times in seconds were: a-0, b-45, c-67.5, d-90, and e-112.

Acknowledgments

We gratefully acknowledge Wigbert Siekhaus for his assistance. This work was performed under the auspices of the U.S. Department of Energy by Lawrence Livermore National Laboratory under contract No. W-7405-Eng-48.

REFERENCES

1. J. Tersoff, A.W. Denier van der Gon, and R.M. Tromp, *Phys. Rev. Lett.* **72**, 266 (1994).
2. M.D. Johnson, C. Orme, A.W. Hunt, D. Graff, J. Sudijono, L.M. Sander, and B.G. Orr, *Phys. Rev. Lett.* **72**, 116 (1994).
3. Y.W. Mo, J. Kleiner, M.B. Webb, and M.G. Lagally, *Phys. Rev. Lett.* **66**, 1998 (1991).
4. J.J. DeYoreo, T.A. Land and B. Dair, *Phys. Rev. Lett.* **73**, 838 (1994).
5. A.J. Gratz, S. Manne and P.K. Hansma, *Science* **251**, 1343 (1991).
6. D.G. Schlom, D. Anselmetti, J.G. Bednorz, R.F. Broom, A. Catana, T. Frey, Ch. Gerber, H.-J. Güntherodt, H.P. Lang, and J. Mannhart, *Z. Phys. B* **86**, 163 (1992).
7. S.D. Durbin and W.E. Carlson, *J. Cryst. Growth* **122**, 71 (1992).
8. A.J. Gratz, P.E. Hillner and P.K. Hansma, *Geochem. et Cosmochim. Acta* **57**, 491 (1993).
9. W.K. Burton, N. Cabrera, and F.C. Frank, *Phil. Trans. Roy. Soc. London A* **243**, 299 (1951).
10. B. Drake, C.B. Prater, A.L. Weisenhorn, S.A.C. Gould, T.R. Albrecht, C.F. Quate, D.S. Cannell, H.G. Hansma and P.K. Hansma, *Science* **243**, 1586 (1989).
11. R.L. Schwoebel and E.J. Shipsey, *J. Appl. Phys.* **37**, 3682 (1966).
12. R. Kunkel, B. Poelsema, L.K. Verheij, G. Comsa, *Phys. Rev. Lett.* **65**, 733 (1990).
13. P.G. Vekilov, Yu.G. Kuznetsov and A.A. Chernov, *J. Cryst. Growth* **121**, 44 and 643 (1992).
14. J.I. Alexander, J.J. DeYoreo and T.A. Land (In progress).
15. O. Söhnel, *J. Cryst. Growth* **57**, 101 (1982).